Plasma Modification of the Surface of Magnesium-nickel alloy: Enhancement of Oxidation Resistance and Optimization of Hydrogen Storage Kinetics

Kai Deng, Jidong Li*
School of Materials and Metallurgy, University of Science and Technology Liaoning, Anshan, 114051, China
Corresponding Author: Jidong Li (lijidong1014@163.com)

Abstract: To address the application bottleneck of magnesium-nickel alloys as hydrogen storage materials, which involves their susceptibility to oxidation and slow hydrogen storage kinetics, this study employed plasma immersion ion implantation technology to modify the surface of Mg_2Ni alloys. The research systematically explored the regulatory laws of process parameters on the surface structure, oxidation resistance, and hydrogen storage kinetics of the alloys. The microstructure of the modified layer was characterized using SEM, XRD, and XPS methods. The performance optimization effect was evaluated through static oxidation experiments, thermogravimetric analysis, and hydrogen absorption/desorption kinetics tests. The results showed that when the plasma treatment power was 400 W, the treatment time was 30 min, and the working pressure was 0.5 Pa, a dense modified layer approximately 2.5 μm thick was formed on the alloy surface, mainly consisting of the composite phase of Ni_3P and MgO. Compared with the unmodified sample, the oxidation rate of the modified alloy in a static oxidation experiment at 600 ℃ for 10 h decreased by 68.3%, and the activation energy of oxidation increased to 186.5 kJ/mol. The hydrogen storage kinetics performance was significantly optimized. At 200 ℃ and 3 MPa hydrogen pressure, the saturated hydrogen absorption time was shortened from 1200 s to 380 s, the hydrogen absorption rate constant increased by 2.1 times, and the storage capacity retention rate after 50 hydrogen absorption/desorption cycles remained at 92.7%, which was 23.5 percentage points higher than that of the unmodified sample. Mechanism analysis indicated that the dense structure of the modified layer could effectively prevent oxygen diffusion to enhance oxidation resistance, while the formation of the Ni_3P catalytic phase and increased surface defects could accelerate the hydrogen adsorption-diffusion process. The proposed plasma modification process provides technical support for the preparation of high-performance magnesium-nickel hydrogen storage alloys and is of great significance for promoting the industrial application of hydrogen storage technology.

Keywords: Magnesium-nickel alloy; Plasma modification; Antioxidant property; Hydrogen storage kinetics; Surface modification

1. Research Significance

Hydrogen energy, as a richly-stored, clean and efficient secondary energy source, is regarded as an important solution to the global energy crisis and environmental problems [1]. However, efficient and safe hydrogen storage technology is the core bottleneck for promoting the industrial application of hydrogen energy. Magnesium-nickel alloys (such as Mg_2Ni) have become a research hotspot in the field of hydrogen storage materials due to their theoretical hydrogen storage capacity of 1.6 wt%, low raw material cost and abundant resource reserves [2]. However, this alloy is prone to oxidation in the air, forming a loose oxide layer, which not only reduces the hydrogen storage capacity but also significantly hinders the adsorption and diffusion of hydrogen atoms, resulting in slow hydrogen storage kinetics and severely limiting its practical application [3]. Surface modification is an effective means to improve the physical and chemical properties of magnesium-nickel alloys. Plasma modification technology, with its high processing efficiency [4], high interface bonding strength, environmental friendliness and the ability to precisely control the surface structure, shows unique advantages in the functional optimization of metal materials surfaces, providing a feasible path to solve the problems of oxidation resistance and hydrogen storage kinetics of magnesium-nickel alloys [5].

Domestic and international scholars have conducted extensive research on the optimization of hydrogen storage performance of magnesium-nickel alloys, proposing various anti-oxidation modification strategies such as coating method, doping method and surface alloying [6]. Although these strategies have improved the alloy performance to a certain extent, they generally have problems such as weak interface bonding, uneven modification effect or complex processes. In terms of plasma modification application, plasma spraying, plasma immersion ion implantation and plasma enhanced chemical vapor deposition have been attempted for the surface modification of hydrogen storage alloys. Studies have shown that plasma treatment can improve the oxidation resistance and hydrogen storage kinetics of alloys by introducing specific phases [7], refining grains or constructing dense layers. However, existing research mostly focuses on the influence of a single process parameter, and the microscopic structure evolution law of the plasma modification layer and its intrinsic relationship with oxidation resistance and hydrogen storage performance are not deeply revealed. Moreover, the optimal plasma modification process parameters combination for magnesium-nickel alloys has not yet formed a unified standard, and the related mechanism still needs to be further systematically explored [8].

Based on the current research status, this study focuses on the Mg_2Ni alloy as the research object and adopts the plasma immersion ion implantation technology for surface modification. The aim is to precisely control the surface structure of the alloy by adjusting the process parameters, and simultaneously enhance its oxidation resistance and hydrogen storage kinetics performance. The main research contents include: optimizing the plasma modification process parameters, characterizing the microstructure, phase composition, and chemical state of the modified alloy surface, systematically testing and analyzing the oxidation resistance and hydrogen storage kinetics performance of the alloy, and revealing the intrinsic mechanism of how plasma modification improves the comprehensive performance of the alloy.

2. Methods

2.1 Experimental Materials and Preparation

The experiment precisely weighed magnesium powder and nickel powder in a 2:1 atomic ratio, with a purity of no less than 99.9%. These powders were dry-ground in a planetary ball mill at a

ball-to-material ratio of 20:1 and a rotational speed of 350 r/min under argon protection for 20 hours to obtain Mg_2Ni alloy powder. Then, the powder was loaded into a graphite mold, hot-pressed and sintered at 450 °C under a vacuum of 20 MPa for 2 hours and cooled in the furnace. The resulting product was shaped into a 10 mm in diameter and 2 mm in thickness circular sheet [9]. After the sample was wet-ground with 400# - 2000# silicon carbide sandpaper to remove the oxide layer, it was finely polished with 1 μm diamond polishing paste to a mirror finish. It was then ultrasonically cleaned in anhydrous ethanol for 15 minutes and vacuum-dried at 60 °C for 2 hours before being stored.

The surface phosphating modification of Mg_2Ni alloy was carried out by using plasma immersion ion implantation technology. The equipment was the HL-800 multi-functional plasma system. The phosphorus source was provided by a mixture of high-purity PH_3 and argon with a volume ratio of 1:10. The experiment fixed the injection voltage at 50 kV and the pulse frequency at 50 Hz. The effects of power ranging from 300 to 500 W [10], time ranging from 10 to 40 min, and gas pressure ranging from 0.3 to 0.7 Pa were systematically investigated in a single-factor rotation manner. Each parameter was changed only while the others remained constant, and a blank control without injection was retained. The chamber was first evacuated to 5×10^{-3} Pa, the mixed gas was introduced until the target pressure was stable for 3 minutes, then the plasma was ignited and the pressure was increased. After the injection was completed, the vacuum was maintained, the sample was cooled to room temperature, and then taken out.

2.2 Surface Microstructure Characterization Methods

The surface and cross-sectional morphologies of the alloys before and after modification were observed using the Su8010 field emission scanning electron microscope at an acceleration voltage of 10 kV [11]. The cross-sectional samples were prepared by ion beam cutting and coupled with an energy spectrometer for elemental distribution analysis. Phase identification was completed on the D8 Advance X-ray diffractometer, using Cu Kα radiation, with a tube voltage of 40 kV, a tube current of 40 mA, a scanning range of 2θ from 20° to 80°, a step size of 0.02°, a scanning speed of 5° per minute. The obtained spectra were analyzed using the Jade 6.0 software to identify the phases and calculate the grain sizes according to the Scherrer formula:

$$D = \frac{K\lambda}{\beta \cos\theta} \tag{1}$$

In the formula: D represents the average grain size (nm); K is the Scherrer constant, which is taken as 0.89; λ is the X-ray wavelength (nm); β is the half-width of the diffraction peak (rad); θ is the diffraction angle (°). Using the ESCALAB 250Xi X-ray photoelectron spectroscopy instrument, with a monochromatic Al Kα ray as the excitation source, and after correcting with the binding energy scale at the C 1s peak at 284.8 eV, the elemental composition and chemical state information of the modified layer were collected. The peak fitting of the spectral peaks was completed with the help of the XPS Peak 4.1 software. The surface nano-morphology and roughness were characterized by the tapping mode of the Dimension Icon atomic force microscope. The scanning area was 5 μm × 5 μm, and the Ra value of each sample was randomly selected from three points and averaged as the final result.

2.3 Antioxidant Performance Testing Method

The static oxidation experiment was conducted using a box-type resistance furnace (model:

SX2-4-10). The test temperature was 600℃, and the oxidation atmosphere was air. The pre-treated samples were precisely weighed (with an accuracy of 0.1 mg) and then placed in an alumina crucible, which was placed in the constant temperature zone of the furnace. The samples were taken out at 2 h, 4 h, 6 h, 8 h, and 10 h of oxidation, cooled to room temperature, and weighed again. The oxidation gain was calculated. The oxidation rate (v) was used to evaluate the antioxidant performance. The oxidation rate was calculated using formula (2):

$$v = \frac{m_t - m_0}{S \cdot t} \tag{2}$$

In the formula: v represents the oxidation rate ($mg \cdot cm^{-2} \cdot h^{-1}$); m_0 is the mass of the sample before oxidation (mg); m_t is the mass of the sample after oxidation for t hours (mg); S is the surface area of the sample (cm^2); t is the oxidation time (h). The dynamic oxidation test was conducted using a synchronous thermal analyzer (model: STA 449 F3) for thermogravimetric (TG) analysis [12]. The test conditions were as follows: air atmosphere, gas flow rate of 50 mL/min, heating rate of 10 ℃/min, temperature range from room temperature to 800 ℃. The curve of sample mass variation with temperature was recorded, and the oxidation kinetics laws were analyzed through the TG curve. The activation energy for oxidation (E_a) was calculated using the Arrhenius formula (Equation 3):

$$v = A\, exp\left(-\frac{E_a}{RT}\right) \tag{3}$$

In the formula: A is the pre-exponential factor ($mg \cdot cm^{-2} \cdot h^{-1}$); R is the gas constant, which is taken as 8.314 $J \cdot mol^{-1} \cdot K^{-1}$; T is the absolute temperature (K). Taking the natural logarithm of both sides of formula (3), a linear relationship between lnv and 1/T is obtained. The slope ($-E_a/R$) is calculated through linear fitting, and then the oxidation activation energy E_a is calculated. The structure and density of the oxide layer of the oxidized sample are observed by SEM, the phase composition of the oxide layer is analyzed by XRD, and combined with the EDS element distribution results, the antioxidant mechanism is revealed.

2.4 Hydrogen Storage Kinetics Performance Testing Method

The hydrogen storage performance test was conducted on the PCT-2000 high-pressure system. Before the test, the samples were degassed at 300°C and a vacuum of $\leq 5 \times 10^{-3}$ Pa for 2 hours to remove surface adsorbed impurities. The pressure-composition-temperature curves were measured within the hydrogen pressure range of 0–3 MPa at 200 °C to obtain the equilibrium hydrogen storage capacity. The hydrogen absorption and desorption kinetics experiments were carried out at a fixed temperature of 200 °C and an initial hydrogen pressure of 3 MPa [13]. The pressure decay curves over time were continuously recorded and the hydrogen absorption amount was converted. Subsequently, the Avrami model was used to fit and analyze the hydrogen absorption kinetics. Analyze the mechanism of hydrogen absorption reaction and calculate the kinetic parameters:

$$ln[-ln(1-\alpha)] = ln\, k + n\, ln\, t \tag{4}$$

In the formula: α represents the hydrogen absorption conversion rate at time t ($\alpha = H_t / H_{max}$, where H_t is the hydrogen absorption amount at time t, and H_{max} is the saturated hydrogen absorption amount); k is the rate constant (s^{-n}); n is the Avrami index, which reflects the control mechanism of the hydrogen absorption reaction (n = 1~2 indicates interface reaction control, and n = 2~3 indicates three-dimensional diffusion control). By plotting ln[-ln(1 - α)] against ln t, a straight line is fitted to obtain the slope n and the intercept ln k, thereby determining the control mechanism of the hydrogen absorption reaction and the rate constant k. The hydrogen activation energy (E_h) is calculated using

the Arrhenius formula. By plotting the ln k and 1/T linear curves at different temperatures (150℃, 200℃, 250℃), the slope is used to calculate the hydrogen activation energy.

3. Results and Discussion

3.1 Microstructural Characteristics of the Plasma-modified Layer of Magnesium-nickel Alloy

The plasma modification process parameters directly control the formation and microstructure of the surface modification layer of magnesium-nickel alloys, thereby influencing the alloy's oxidation resistance and hydrogen storage performance. This section systematically analyzes the microscopic characteristics of the modification layer and the regulation rules of the process parameters from four dimensions: surface morphology, phase composition, chemical state, and cross-sectional structure. The schematic diagram of magnesium alloy under different plasma treatment powers is shown in Figure 1.

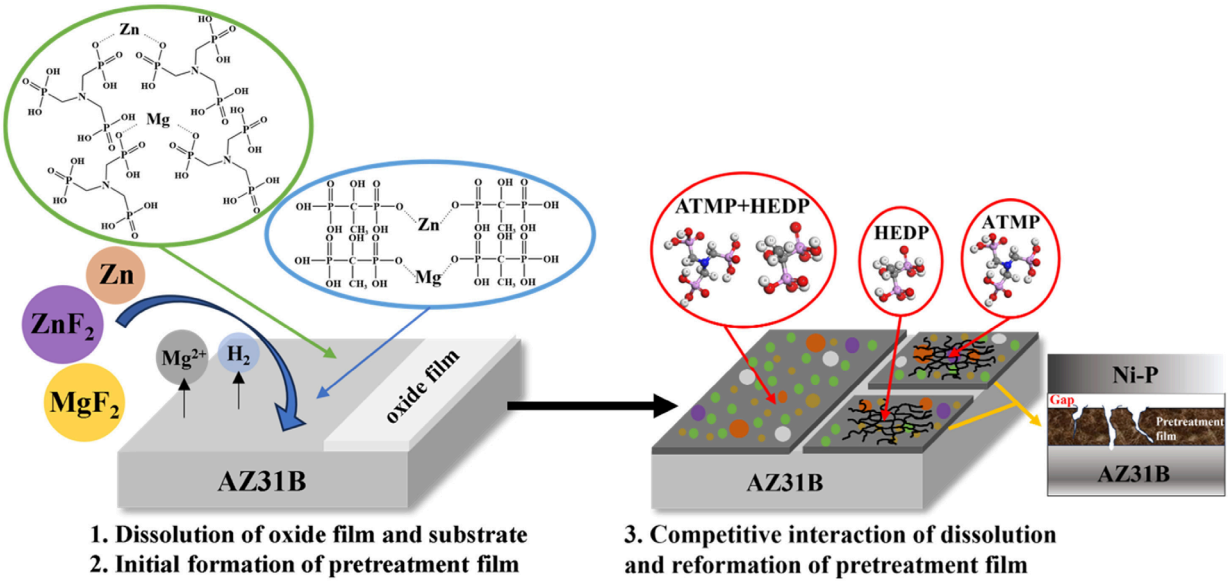

Figure 1: Schematic Diagram of Mg_2Ni alloy Under Different Plasma Treatment Powers.

Table 1 presents the surface roughness (Ra) and grain size data of the modified layer under different process parameters. From the table, it can be seen that as the processing time increased from 10 minutes to 30 minutes, the Ra value decreased from 59.2 nm to 38.9 nm, and the grain size decreased from 45.3 nm to 28.6 nm; further extending the time to 40 minutes, the changes in Ra value and grain size were not significant. The working pressure also has an impact on the surface structure. At 0.5 Pa, the modified layer obtained the smallest Ra value (38.9 nm) and the finest grain size (28.6 nm), while at 0.3 Pa and 0.7 Pa, the surface roughness increased. This is because an appropriate processing time and working pressure can ensure the stability of the plasma, promote uniform ion injection and surface grain refinement; too long processing time or deviating from the optimal pressure will result in uneven ion distribution and affect the uniformity of the modified layer. The surface of the magnesium-nickel alloy under the scanning electron microscope is shown in Figure 2.

Table 1: Surface Roughness and Grain Size of the Modified Layer Under Different Process Parameters.

Processing	Processing	Working	Surface	Grain

Power (W)	Time (min)	Pressure (Pa)	Roughness Ra (nm)	Size (nm)
Unmodified	-	-	85.6±3.2	62.5±4.1
300	30	0.5	62.3±2.5	39.8±3.5
400	10	0.5	59.2±2.8	45.3±3.8
400	20	0.5	45.7±2.1	35.2±2.9
400	30	0.5	38.9±1.8	28.6±2.2
400	40	0.5	39.2±1.9	27.8±2.0
400	30	0.3	52.6±2.4	33.5±2.6
400	30	0.7	48.8±2.3	31.2±2.4
500	30	0.5	76.1±3.0	36.9±3.2

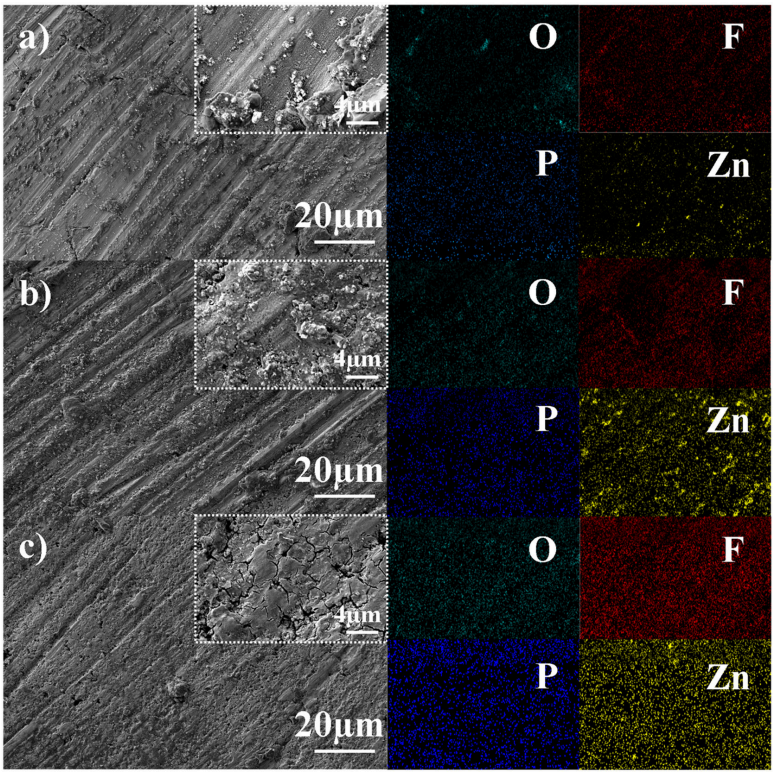

Figure 2: The surface of the Magnesium-Nickel Alloy Under the Scanning Electron Microscope.

Figure 3 shows the XRD patterns of the unmodified Mg_2Ni alloy and the Mg_2Ni alloy under different processing parameters. The diffraction peaks of the unmodified sample correspond to the Mg_2Ni phase (PDF#35-0891), and the peaks are sharp, indicating good crystallinity. After plasma modification, new diffraction peaks appeared, corresponding to the Ni_3P phase (PDF#65-3544) and the MgO phase (PDF#45-0946), and as the processing power increased, the intensities of the Ni_3P and MgO phase diffraction peaks first increased and then decreased, reaching the maximum at 400 W; when the processing time was extended to 30 minutes, the diffraction peak intensities tended to stabilize. This is because during the plasma treatment process, the injected phosphorus ions react chemically with the nickel elements in the matrix to form the Ni_3P phase, and a small amount of magnesium on the surface reacts with the residual oxygen in the vacuum chamber to form the MgO phase. When the power is too high (500 W), the local high temperature causes slight decomposition of

the Ni_3P phase, resulting in a decrease in the diffraction peak intensity.

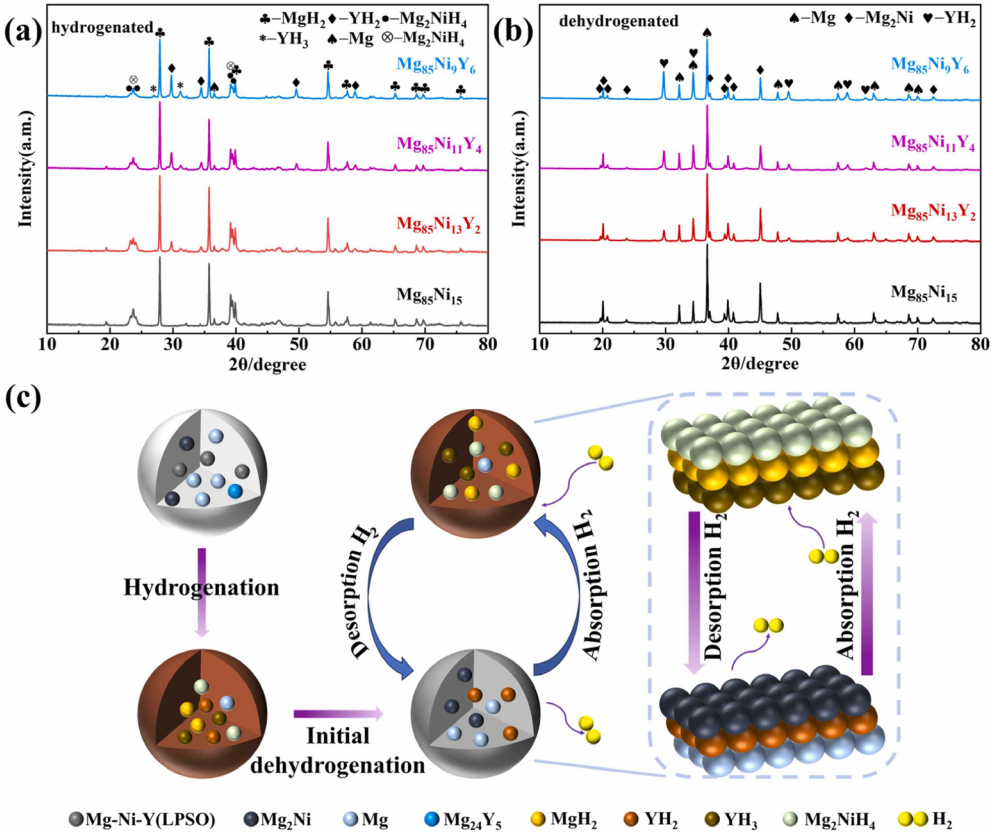

Figure 3: XRD Patterns of Mg_2Ni Alloy Under Different Processing Parameters.

Table 2 lists the relative contents of the phases in the modified layer under different processes. Under the optimal process, the relative content of the Ni_3P phase is 28.6%, the relative content of the MgO phase is 12.3%, and the relative content of the Mg_2Ni matrix phase is 59.1%. The Ni_3P phase is a good hydrogen storage catalytic phase, which can accelerate the dissociation and diffusion of hydrogen molecules; the MgO phase has good chemical stability and can prevent the penetration of oxidizing media. The coexistence of these two phases provides a phase basis for the improvement of alloy performance.

Table 2: The Relative Content of Phase Compositions in the Modified Layer Under Different Processes.

Process Parameters	Relative Content of Mg_2Ni Phase (%)	Relative Content of Ni_3P Phase (%)	Relative Content of MgO Phase (%)
Unmodified	100.0	-	-
300 W, 30 min, 0.5 Pa	72.5	18.3	9.2
400 W, 30 min, 0.5 Pa	59.1	28.6	12.3
500 W, 30 min, 0.5 Pa	68.3	21.5	10.2
400 W, 40 min, 0.5 Pa	58.7	29.1	12.2

3.2 The influence and mechanism of plasma modification on the oxidation resistance of

magnesium-nickel alloys

Figure 4 shows the static oxidation kinetics curves of Mg_2Ni alloy before and after modification under different process parameters at different temperatures in air. The weight gain of the unmodified sample increased rapidly with time, reaching 12.8 $mg \cdot cm^{-2}$ at 10 hours; after plasma modification, the weight gain decreased significantly, and with the optimization of processing power and time, the weight gain gradually decreased, reaching the minimum value of 3.8 $mg \cdot cm^{-2}$ under the optimal process. The oxidation rate of the unmodified sample was 1.28 $mg \cdot cm^{-2} \cdot h^{-1}$, and the activation energy was 108.6 $kJ \cdot mol^{-1}$; under the optimal process, the oxidation rate of the modified sample decreased to 0.39 $mg \cdot cm^{-2} \cdot h^{-1}$, which was 68.3% lower than that of the unmodified sample, and the activation energy increased to 186.5 $kJ \cdot mol^{-1}$, indicating that the oxidation resistance of the modified alloy was significantly enhanced. The optimization of hydrogen storage kinetics performance of magnesium-nickel alloy through plasma modification and the underlying mechanism are shown in Figure 5.

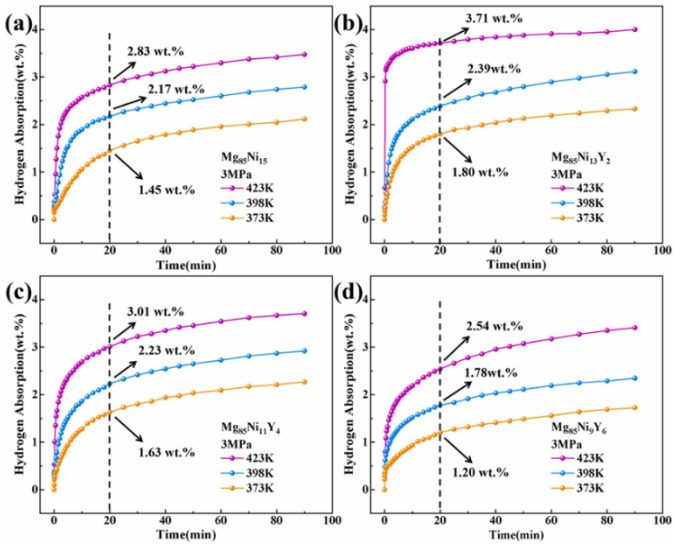

Figure 4: The Static Oxidation Kinetic Curves of Mg_2Ni Alloy Under Different Process Parameters in Air.

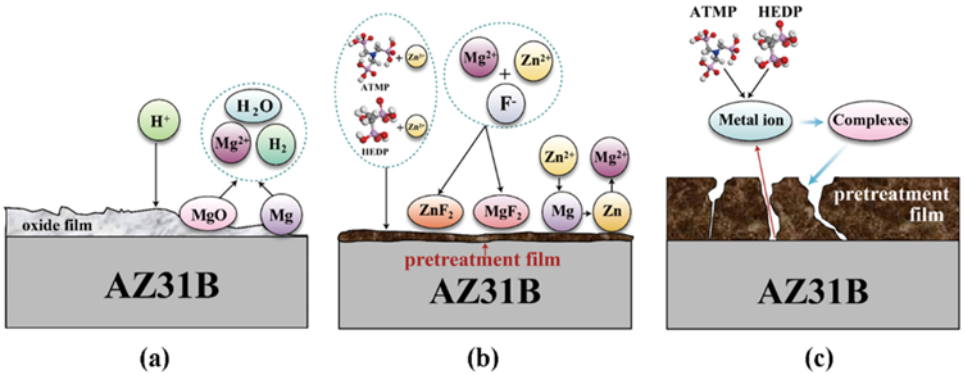

Figure 5: Plasma Modification for Optimizing the Hydrogen Storage Kinetics Performance of Magnesium-nickel Alloys and its Mechanism.

The hydrogen absorption rate of the unmodified sample was slow, and the time required to reach the saturated hydrogen absorption capacity was 1200 seconds, with the saturated hydrogen absorption capacity being 1.45 wt%. After plasma modification, the hydrogen absorption rate

significantly increased, and the saturated hydrogen absorption time was shortened. Under the optimal process, the saturated hydrogen absorption time was only 380 seconds, which was 68.3% shorter than that of the unmodified sample, and the saturated hydrogen absorption capacity increased to 1.58 wt%. The hydrogen absorption kinetics curve was fitted using the Avrami kinetic model. The hydrogen absorption rate constant k of the unmodified sample was 0.0021 s^{-1}, and the Avrami index n was 2.6, indicating that the hydrogen absorption reaction was controlled by three-dimensional diffusion; under the optimal process, the k value of the modified sample increased to 0.0065 s^{-1}, which was 2.1 times higher than that of the unmodified sample, and the n value was 2.2, still being controlled by three-dimensional diffusion, but the diffusion resistance was significantly reduced.

4. Conclusion

This study employed plasma immersion ion implantation technology to modify the surface of Mg_2Ni alloy. It systematically explored the regulatory laws of process parameters on the surface structure and comprehensive properties of the alloy, clarified the mechanism of performance improvement and determined the optimal process scheme. The research results showed that when the processing power was 400 W, the processing time was 30 min, and the working gas pressure was 0.5 Pa, a dense Ni_3P and MgO composite modification layer with a thickness of approximately 2.5 μm could be formed on the alloy surface. Under this process, the alloy's comprehensive performance was the best: the oxidation rate at 600 ℃ under static oxidation for 10 h was 68.3% lower than that of the unmodified sample, and the oxidation activation energy increased to 186.5 kJ/mol; the saturated hydrogen absorption time at 200 ℃ and 3 MPa hydrogen pressure was shortened from 1200 s to 380 s, the hydrogen absorption rate constant increased by 2.1 times, and the storage capacity after 50 hydrogen absorption and release cycles reached 92.7%, which was 23.5 percentage points higher than that of the unmodified sample. Mechanism analysis confirmed that the dense modification layer could effectively prevent oxygen diffusion to enhance oxidation resistance, while the Ni_3P catalytic phase and the large number of grain boundaries formed due to surface grain refinement could accelerate the dissociation and diffusion process of hydrogen molecules. The plasma modification process and surface structure-performance correlation mechanism clearly defined in this study provided reliable technical support for the preparation of high-performance magnesium-nickel hydrogen storage alloys, and is of great significance for promoting the industrialization of hydrogen storage technology. At the same time, this study did not verify the long-term service stability of the modification layer and the performance under actual complex conditions. In the future, further research on multivariate plasma co-modification and exploration of the scale application path of the modification process can be carried out to expand the practical application scenarios of magnesium-nickel alloys.

References

[1] Kang, Y., Zhang, K., & Lin, X. (2023). Surface modifications of magnesium-based materials for hydrogen storage and nickel–metal hydride batteries: a review. Coatings, 13(6), 1100.

[2] Mose, M. P., & Huang, S. J. (2024). Enhanced hydrogen storage capacity and kinetics in AZ61 alloy with nickel and cobalt additives: Insights into reaction mechanisms and activation energy. Journal of Alloys and Compounds, 984, 173934.

[3] Wang, Y., & Yang, X. (2025). Cloud computing energy consumption prediction based on kernel extreme

learning machine algorithm improved by vector weighted average algorithm. In Proceedings of the 2025 5th International Conference on Artificial Intelligence and Industrial Technology Applications (AIITA) (pp. 1355–1361).

[4] Hu, X., Tang, T., Tan, L., & Zhang, H. (2023, October). Fault detection for point machines: A review, challenges, and perspectives. In Actuators (Vol. 12, No. 10, p. 391). MDPI.

[5] Huang, Y., Huang, W., Hu, X., Liu, Z., & Huo, J. (2025). UDDGN: Domain-Independent Compact Boundary Learning Method for Universal Diagnosis Domain Generation. IEEE Transactions on Instrumentation and Measurement.

[6] Li, L., Huang, P., Wang, T., & Zeng, G. (2021). Practical security of a chip-based continuous-variable quantum-key-distribution system. Physical Review A, 103(3), 032611.

[7] Hao, L., Jin, C., Gao, X., Wu, F., & Chen, G. (2017, December). Towards cost-effective and budget-balanced task allocation in crowdsourcing systems. In 2017 IEEE 36th International Performance Computing and Communications Conference (IPCCC) (pp. 1-8). IEEE.

[8] Xu, Y., Zhou, Y., Li, Y., Hao, Y., Wu, P., & Ding, Z. (2024). Recent advances in the preparation methods of magnesium-based hydrogen storage materials. Molecules, 29(11), 2451.

[9] Wu, L., & Wang, S. (2025). Development of a virtual reality creative enhancement system utilizing haptic vibration feedback via electroencephalography. Education and Information Technologies, 30(5), 5727-5753.

[10] Sun, W., Sun, H., Zhang, X., Sheng, P., Li, J., & Zhang, Y. (2025). Improved Hydrogen Storage Thermodynamics and Kinetics of As-Milled Ce-Mg-Ni-Based Alloys by Adding Ni. Journal of Materials Engineering and Performance, 34(10), 8669-8682.

[11] Zhao, F., Huang, B., Wang, J., et al. (2025). Seafloor debris detection using underwater images and deep learning-driven image restoration: A case study from Koh Tao, Thailand. Marine Pollution Bulletin, 214, 117710.

[12] Qinglin Meng, Sheharyar Hussain, Fengzhang Luo et al. An Online Reinforcement Learning-based Energy Management Strategy for Microgrids with Centralized Control. IEEE Transactions on Industry Applications, 2025, 61(1), 1501-1510. DOI: 10.1109/TIA.2024.3430264.

[13] Safyari, M., Gneiger, S., Simson, C., & Moshtaghi, M. (2024). A new methodology for extra enhancement of hydrogen storage capacity of Mg–Ni based alloys: The role of gaseous O2/H2 mixture. International Journal of Hydrogen Energy, 73, 761-767.